

Oriented Matroid Circuit Polytopes

Laura Escobar* and Jodi McWhirter†

January 3, 2025

Abstract

Matroids give rise to several natural constructions of polytopes. Inspired by this, we examine polytopes that arise from the signed circuits of an oriented matroid. We give the dimensions of these polytopes arising from graphical oriented matroids and their duals. Moreover, we consider polytopes constructed from cocircuits of oriented matroids generated by the positive roots in any type A root system. We give an explicit description of their face structure and determine the Ehrhart series. We also study an action of the symmetric group on these polytopes, giving a full description the subpolytopes fixed by each permutation. These type A polytopes are graphic zonotopes, are polar duals of symmetric edge polytopes, and also make an appearance in Stapledon’s paper introducing Equivariant Ehrhart Theory.

1 Introduction

Polytopes have been a key object in the study of matroids. There are various ways that one can construct a polytope from a matroid. Since such polytopes are arithmetically interesting, see e.g. [9], Matthias Beck posed the question in 2021 to study the arithmetic of polytopes constructed from the indicator vectors of the signed circuits of an oriented matroid. We study these oriented matroid circuit (OMC) polytopes. Using the circuit axioms, we show that every circuit yields a vertex of the corresponding OMC polytope and that every OMC polytope is centrally symmetric. Turning to graphical and co-graphical oriented matroids, we determine the dimension of the corresponding OMC polytopes. We also describe the effect that some special graph edges, namely bridges and loops, have on the OMC polytope.

We give more detailed information on a family of OMC polytopes that arise from the classical type A_n root system, which we call \mathcal{P}_n . Aside from being an OMC polytope, \mathcal{P}_n appears in other families of polytopes. For instance, we show that it is affinely isomorphic to the graphic zonotope $\mathcal{Z}_{C_{n+1}}$, where C_{n+1} is the cycle graph on $n + 1$ nodes. It is also a tropical unit ball, as seen in [6], which is the polar dual of the symmetric edge polytope for the complete graph K_{n+1} . We describe the face structure of \mathcal{P}_n .

We also study the Ehrhart theory of \mathcal{P}_n . Moreover, the symmetric group S_{n+1} action on the graph K_{n+1} induces an S_{n+1} action on the vertices of \mathcal{P}_n . We describe each subpolytope \mathcal{P}_n^σ of points of \mathcal{P}_n that are fixed by a $\sigma \in S_{n+1}$. These fixed polytopes fit in the larger picture of equivariant Ehrhart theory, introduced by Stapledon in [17]. It is of recent interest to compute the equivariant Ehrhart theory of polytopes that admit a group action, see e.g. [2, 3, 5, 12], in part due to a conjecture by Stapledon [17, Conjecture 12.1]. In fact, \mathcal{P}_n also appears in [17], where Stapledon connects its equivariant Ehrhart theory to the cohomology of the toric variety of the permutahedron. We use the fixed polytopes of \mathcal{P}_n to compute the equivariant Ehrhart theory in a different way.

A natural question is to study these polytopes for other Coxeter types. First, we observe that types B_n and C_n yield the same polytopes: since signed circuits encode the positive and negative coefficients of linear dependencies of vectors, the set of signed circuits of $\mathcal{M}(B_n)$ and $\mathcal{M}(C_n)$ are the same, resulting in the same OMC polytopes. While it would be interesting to study the OMC polytopes of these other Coxeter types,

*Washington University in St. Louis; laurae@wustl.edu.

†Washington University in St. Louis; jodi.mcwhirter@wustl.edu.

these polytopes are very high-dimensional in types B_n/C_n and D_n , as referenced in Example 2.9, which leads to some challenges.

We now give an outline of the paper. In Section 2, we introduce some background on oriented matroids and define oriented matroid circuit (OCM) polytopes in Definition 2.2. Proposition 2.7 and Proposition 2.8 give the dimension of the OMC polytope for graphical and co-graphical oriented matroids, respectively.

Section 3 examines the OMC polytope \mathcal{P}_n coming from the family of oriented matroid dual to those determined by the positive roots of the type A_n root system. This family is also co-graphical, being also dual to the graphical oriented matroids determined by the complete graph K_{n+1} . In Section 3.2, we find \mathcal{P}_n in the context of graphic zonotopes [14] and symmetric edge polytopes [8]. Theorem 3.5 and Corollary 3.6 in Section 3.3 connect the face structure of \mathcal{P}_n to the Boolean lattice on $[n+1]$.

In Section 3.4, we study the Ehrhart theory of \mathcal{P}_n , which is given specifically in Proposition 3.9. Sections 3.5 and 3.6 concern equivariant Ehrhart theory. In Section 3.5, we fully describe the S_{n+1} -action on \mathcal{P}_n and, in Theorem 3.11, the polytopes \mathcal{P}_n^σ fixed by each $\sigma \in S_{n+1}$. Using these fixed polytopes, Corollary 3.12 gives explicitly the equivariant H^* -series of \mathcal{P}_n under our S_{n+1} action. Finally, in Section 3.6, we compare the fixed polytopes of our S_{n+1} action on \mathcal{P}_n to the fixed polytopes of a different group action coming from graphic zonotopes.

2 Oriented matroid circuit polytopes

We begin by giving the background on oriented matroids, following [4, Section 3]. A **signed set** \tilde{X} is a set X together with a partition (X^+, X^-) of X . The **opposite** of \tilde{X} is the signed set $-\tilde{X} = ((-X)^+, (-X)^-)$ with $(-X)^+ := X^-$ and $(-X)^- := X^+$.

Definition 2.1. *A set \mathcal{C} of signed sets is the set of **circuits** of an **oriented matroid** if the following hold:*

- (C0) *The empty signed set (\emptyset, \emptyset) is not a circuit*
- (C1) *If \tilde{X} is a circuit, then so is $-\tilde{X}$*
- (C2) *For all $\tilde{X}, \tilde{Y} \in \mathcal{C}$, if $X \subseteq Y$, then $\tilde{X} = \tilde{Y}$ or $\tilde{X} = -\tilde{Y}$*
- (C3) *If \tilde{X}, \tilde{Y} are circuits with $\tilde{X} \neq -\tilde{Y}$ and $e \in X^+ \cap Y^-$, then there is a third circuit \tilde{Z} such that $Z^+ \subseteq (X^+ \cup Y^+) \setminus \{e\}$ and $Z^- \subseteq (X^- \cup Y^-) \setminus \{e\}$.*

In the literature, these “circuits” are often referred to as “signed circuits”; since we are rarely dealing with unsigned circuits, we will just use “circuits.”

Representable oriented matroids are given by lists of vectors in a vector space as follows. Let \mathbb{K} be a totally ordered field. Given a matrix $M \in \mathbb{K}^{d \times n}$ with column vectors $\mathbf{v}_1, \dots, \mathbf{v}_n$, one associates an oriented matroid as follows. A linear dependence of M is $(\lambda_1, \dots, \lambda_n) \in \mathbb{K}^n$ such that $\sum_{i=1}^n \lambda_i \mathbf{v}_i = 0$. A linear dependence is minimal if there is no linear dependence $(\lambda'_1, \dots, \lambda'_n)$ such that

$$\{i \in [n] \mid \lambda'_i \neq 0\} \subsetneq \{i \in [n] \mid \lambda_i \neq 0\}.$$

Given a minimal linear dependence $(\lambda_1, \dots, \lambda_n) \in \mathbb{K}^n$ we associate the signed set $\tilde{X} = (X^+, X^-)$ given by

$$X^+ = \{i \in [n] \mid \lambda_i > 0\}, \quad X^- = \{i \in [n] \mid \lambda_i < 0\}.$$

The circuits of the oriented matroid $\mathcal{M}(M)$ consist of the signed sets associated to minimal linear dependencies. Moreover, an oriented matroid \mathcal{M} is **representable over** \mathbb{K} if $\mathcal{M} = \mathcal{M}(M)$ for some matrix M with entries in \mathbb{K} .

For example, consider the matrix

$$M = \begin{pmatrix} 0 & -1 & -1 & 0 & 0 & 0 \\ 14 & -1 & -9 & 0 & 0 & 0 \\ 1 & 5 & -1 & 1 & 0 & 1 \end{pmatrix}.$$

We use the numbers $1, 2, \dots, 6$ to denote the columns of the matrix and, to simplify notation, often use, for instance, 136 to denote $\{1, 3, 6\}$. The circuits of $\mathcal{M}(M)$ are $(5, \emptyset)$, $(\emptyset, 5)$, $(4, 6)$, $(6, 4)$, $(134, 2)$, $(2, 134)$, $(136, 2)$, $(2, 136)$. Another way to denote circuits is through strings of $+$ s, $-$ s, and 0 s. For example, the circuit $(134, 2)$ would be written as $(+, -, +, +, 0, 0)$.

As a second example, consider the matrix

$$M = \begin{pmatrix} 1 & 1 & 1 & 1 & 0 & 0 \\ 1 & -1 & 0 & 0 & 1 & 1 \\ 0 & 0 & 1 & -1 & 1 & -1 \end{pmatrix},$$

whose columns are the type \mathcal{D}_3 positive roots. The oriented matroid $\mathcal{M}(\mathcal{D}_3)$ corresponding to the matrix M has 14 circuits, including $(1, 36)$ and $(36, 45)$.

Let us describe the notion of a dual oriented matroid in the context of representable matroids. The oriented matroid $\mathcal{M}^*(M)$ which is dual to $\mathcal{M}(M)$ is given as follows. Given $\mathbf{u} \in \text{rowsp}(M)$, the **signed support** of \mathbf{u} is the signed set $\tilde{X} = (X^+, X^-)$ where

$$X^+ = \{i \in [n] \mid u_i > 0\}, \quad X^- = \{i \in [n] \mid u_i < 0\}.$$

The circuits of $\mathcal{M}^*(M)$ are the inclusion-minimal non-empty signed supports of the vectors in $\text{rowsp}(M)$, see e.g. [10, Lemmas 4.1.34 and 4.1.38].

2.1 Oriented matroid circuit polytopes

Having introduced the necessary background, we are now ready to define the polytopes we study. Let \mathcal{M} be an oriented matroid with circuit set \mathcal{C} . For $\tilde{X} \in \mathcal{C}$, define the **signed incidence vector** $\mathbf{v}_{\tilde{X}}$ by

$$(\mathbf{v}_{\tilde{X}})_j := \begin{cases} 0, & j \notin \tilde{X} \\ 1, & j \in X^+ \\ -1, & j \in X^- \end{cases}.$$

Definition 2.2. The **oriented matroid circuit (OMC) polytope** $P_{\mathcal{M}}$ associated to the matroid \mathcal{M} with nonempty circuit set \mathcal{C} is the convex hull of all such $\mathbf{v}_{\tilde{X}}$, that is,

$$P_{\mathcal{M}} = \text{conv}\{\mathbf{v}_{\tilde{X}} \mid \tilde{X} \in \mathcal{C}\}.$$

Remark 2.3. Let \mathcal{M} be an oriented matroid with ground set E . By [4, Remark 3.2.3], given $A \subseteq E$ we can consider the oriented matroid \mathcal{M}' obtained by reversing the orientation of the elements of A . Note that the linear map

$$\mathbb{R}^E \rightarrow \mathbb{R}^E, \quad x_e \mapsto \begin{cases} -x_e, & e \in A \\ x_e, & e \notin A \end{cases}$$

witnesses that $P_{\mathcal{M}}$ and $P_{\mathcal{M}'}$ are unimodularly equivalent polytopes. Also, note that if \mathcal{M}_1 and \mathcal{M}_2 are oriented matroids with circuits $\mathcal{C}_1, \mathcal{C}_2$ and disjoint, then $P_{\mathcal{M}_1 \oplus \mathcal{M}_2} = P_{\mathcal{M}_1} \times P_{\mathcal{M}_2}$. Here, $\mathcal{M}_1 \oplus \mathcal{M}_2$ denotes the direct sum of the matroids, i.e. the oriented matroid with circuits $\mathcal{C}_1 \cup \mathcal{C}_2$.

Proposition 2.4. The vertices of $P_{\mathcal{M}}$ are precisely those $\mathbf{v}_{\tilde{X}}$ such that \tilde{X} is a circuit of \mathcal{M} .

Proof. Suppose \mathcal{M} is an oriented matroid, \mathcal{C} is its set of circuits, $V = \{\mathbf{v}_{\tilde{X}} \mid \tilde{X} \in \mathcal{C}\}$, and P is the OMC polytope. We would like to show that each $\mathbf{v}_{\tilde{X}} \in V$ is a vertex of P .

Let $\tilde{X} \in \mathcal{C}$ be a circuit with $X^+ = \{a_1, \dots, a_k\}$ and $X^- = \{b_1, \dots, b_l\}$. Now, consider $x \in P$. If we take the dot product of x with the direction vector $\mathbf{v}_{\tilde{X}}$, we get

$$\begin{aligned} \mathbf{v}_{\tilde{X}} \cdot x &= (u_{a_1} x_{a_1} + \dots + u_{a_k} x_{a_k}) + (u_{b_1} x_{b_1} + \dots + u_{b_l} x_{b_l}) \\ &= (x_{a_1} + \dots + x_{a_k}) - (x_{b_1} + \dots + x_{b_l}) \\ &\leq k + l \end{aligned}$$

since $|x_m| \leq 1$. If $x = \mathbf{v}_{\tilde{X}}$, then $\mathbf{v}_{\tilde{X}} \cdot x = \mathbf{v}_{\tilde{X}} \cdot \mathbf{v}_{\tilde{X}} = k + l$. In particular, $\mathbf{v}_{\tilde{X}}$ is maximized by $\mathbf{v}_{\tilde{X}}$ and thus lies on a face of P . Now, consider $\tilde{Y} \in \mathcal{C}$ and suppose $\mathbf{v}_{\tilde{X}} \cdot \mathbf{v}_{\tilde{Y}} = k + l$ as well. It follows that $X^+ \subseteq Y^+$ and $X^- \subseteq Y^-$. Thus $X \subseteq Y$. By circuit axiom (C2), this implies $\tilde{X} = \tilde{Y}$. In particular, $\mathbf{v}_{\tilde{X}}$ is a vertex of P . \square

The following is immediate.

Corollary 2.5. *For any oriented matroid \mathcal{M} , the polytope $P_{\mathcal{M}}$ is centrally symmetric, i.e. $x \in P_{\mathcal{M}}$ implies $-x \in P_{\mathcal{M}}$.*

Remark 2.6. Note that since $\mathcal{P}_{\mathcal{M}}$ is centrally symmetric, the origin lies in its interior so that its dimension equals the dimension of the vector space spanned by its vertices. Some facts are known about this dimension, see e.g. [4, Exercise 4.45]. As a consequence, for any oriented matroid with ground set E and rank r , $\dim(\mathcal{P}_{\mathcal{M}}) \geq |E| - r$. However, it is an open problem to find the dimension of this vector space for general oriented matroids.

2.2 Graphical oriented matroid circuit polytopes

In this section we concentrate on graphical oriented matroids. Given a graph $G = (V, E)$ let \tilde{G} be a directed graph obtained by orienting each edge of G . The circuits of the oriented matroid $\mathcal{M}(\tilde{G})$ are obtained from the cycles of G as follows. Given a cycle C of G , choose a way to traverse C . We obtain the circuits $\tilde{C} = (C^+, C^-)$ and $-\tilde{C}$ by setting

$$\begin{aligned} C^+ &:= \{e \in E \mid e \text{ is traversed following its orientation}\} \\ C^- &:= \{e \in E \mid e \text{ is traversed opposite to its orientation}\}. \end{aligned}$$

The circuits of $\mathcal{M}(\tilde{G})$ are obtained by constructing the circuits above for all cycles of G . It is well known that $\mathcal{M}(\tilde{G})$ is represented over any ordered field by its incidence matrix.

For example, consider the graph in Figure 1. The oriented matroid $\mathcal{M}(\tilde{K}_3)$ has two circuits: $(\{\vec{12}, \vec{23}\}, \{\vec{13}\})$

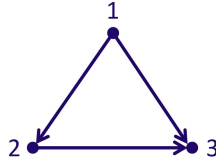


Figure 1: The complete graph \tilde{K}_3 on 3 nodes, oriented so that the arrow points at the larger number.

and $(\{\vec{13}\}, \{\vec{12}, \vec{23}\})$, which can also be represented, under the indexing $(\vec{12}, \vec{13}, \vec{23})$, as $(+, -, +)$ and $(-, +, -)$. The OMC polytope $P_{\mathcal{M}(\tilde{K}_3)}$ is therefore a line segment in \mathbb{R}^3 .

We now give the dimension of $P_{\mathcal{M}(\tilde{G})}$.

Proposition 2.7. *Let $G = (V, E)$ be a graph and \tilde{G} be a directed graph obtained by orienting each edge of G . The dimension of $P_{\mathcal{M}(\tilde{G})}$ is $|E| - |V| + k$, where k is the number of connected components of G .*

Proof. As discussed in Remark 2.6, we want to compute the dimension of the vector space spanned by the vertices of $P_{\mathcal{M}(\tilde{G})}$. By [4, Exercies 4.45], this dimension is $|E| - r$, where r is the rank of $\mathcal{M}(\tilde{G})$. The proposition follows, since the rank of $\mathcal{M}(\tilde{G})$ equals the number of edges in a spanning forest, i.e. $r = |V| - k$. \square

2.3 Graphical oriented matroid cocircuit polytopes

Let $G = (V, E)$ be a graph. The following can be found in [4, § 1.1]. A **minimal cut** of G is a partition $V = V_1 \sqcup V_2$ such that deleting all edges in G between V_1 and V_2 increases by one the number of connected components of G . Let \tilde{G} be a directed graph obtained by orienting each edge of G . We now describe how to obtain a matroid $\mathcal{M}^*(\tilde{G})$, which is dual to the matroid $\mathcal{M}(\tilde{G})$ of Section 2.2, from the minimal cuts of G . The circuits of the oriented matroid $\mathcal{M}^*(\tilde{G})$ are obtained from the minimal cuts of G as follows. Given a minimal cut $V = V_1 \sqcup V_2$ of G , we obtain the circuits $\tilde{C} = (C^+, C^-)$ and $-\tilde{C}$ by setting

$$\begin{aligned} C^+ &:= \{e \in E \mid e \text{ goes from } V_1 \text{ to } V_2\} \\ C^- &:= \{e \in E \mid e \text{ goes from } V_2 \text{ to } V_1\}. \end{aligned}$$

The circuits of $\mathcal{M}^*(\tilde{G})$ are obtained by constructing the circuits above for all minimal cuts of G .

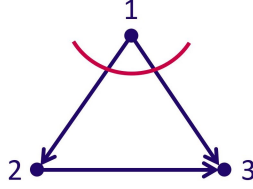


Figure 2: A cut of \tilde{K}_3 with $V_1 = \{1\}$ and $V_2 = \{2, 3\}$. This depicts the cocircuits $(\{\vec{12}, \vec{13}\}, \emptyset)$ and $(\emptyset, \{\vec{12}, \vec{13}\})$.

To continue the example of \tilde{K}_3 , the cocircuits of $\mathcal{M}(\tilde{K}_3)$ are $(\{\vec{12}, \vec{13}\}, \emptyset)$, $(\emptyset, \{\vec{12}, \vec{13}\})$, $(\{\vec{12}\}, \{\vec{23}\})$, $(\{\vec{23}\}, \{\vec{12}\})$, $(\{\vec{13}, \vec{23}\}, \emptyset)$, and $(\emptyset, \{\vec{13}, \vec{23}\})$, which can also be written as $(+, +, 0)$, $(-, -, 0)$, $(+, 0, -)$, $(-, 0, +)$, $(0, +, +)$, and $(0, -, -)$. The OMC polytope $P_{\mathcal{M}^*(\tilde{K}_3)}$ is a hexagon in \mathbb{R}^3 , pictured in Figure 3.

Proposition 2.8. *Let $G = (V, E)$ be a graph and \tilde{G} be a directed graph obtained by orienting the edges of G . The dimension of $P_{\mathcal{M}^*(\tilde{G})}$ is $|V| - k$, where k is the number of connected components of G .*

Proof. The incidence matrix A of \tilde{G} represents $\mathcal{M}(\tilde{G})$ over any ordered field. It follows that the circuits \mathcal{C}^* of $\mathcal{M}^*(\tilde{G})$ are the inclusion-minimal non-empty signed supports of the vectors in $\text{rowsp}(A)$. We wish to compute the dimension of the vector space spanned by $\{\mathbf{v}_{\tilde{X}} \mid \tilde{X} \in \mathcal{C}^*\}$.

Note that the row of A corresponding to the node $i \in V$ is precisely $\mathbf{v}_{\tilde{C}}$, where \tilde{C} is the circuit corresponding to the cut $V = \{i\} \sqcup (V \setminus \{i\})$. It follows that $\text{rowsp}(A) \subseteq \text{span}\{\mathbf{v}_{\tilde{X}} \mid \tilde{X} \in \mathcal{C}^*\}$. We now prove the opposite inclusion. Let $V = V_1 \sqcup V_2$ be a minimal cut of G and \tilde{X} the corresponding circuit. For each node $i \in V$, denote by \tilde{C}_i the circuit corresponding to the cut $V = \{i\} \sqcup (V \setminus \{i\})$. We claim that

$$\mathbf{v}_{\tilde{X}} = \sum_{i \in V_1} \mathbf{v}_{\tilde{C}_i}. \quad (2.1)$$

Suppose that $e = (j, k) \notin X$ so that $(\mathbf{v}_{\tilde{X}})_e = 0$ and note that either $j, k \in V_1$ or $j, k \in V_2$. In the first case, we have

$$\sum_{i \in V_1} (\mathbf{v}_{\tilde{C}_i})_e = (\mathbf{v}_{\tilde{C}_j})_e + (\mathbf{v}_{\tilde{C}_k})_e = 1 - 1 = 0.$$

The second case follows from $(\mathbf{v}_{\tilde{C}_i})_e = 0$ for all $i \in V_1$. Next, suppose that $e = (j, k) \in X^+$ and note that

$$(\mathbf{v}_{\tilde{X}})_e = 1 = (\mathbf{v}_{\tilde{C}_j})_e = \sum_{i \in V_1} (\mathbf{v}_{\tilde{C}_i})_e.$$

The case $e \in X^-$ follows from similar reasoning. It follows that (2.1) holds and thus $\text{rowsp}(A) = \text{span}\{\mathbf{v}_{\tilde{X}} \mid \tilde{X} \in \mathcal{C}^*\}$. We conclude that $\dim(P_{\mathcal{M}^*(\tilde{G})}) = \text{rank}(A) = |V| - k$. \square

Together, Proposition 2.7 and Proposition 2.8 give us that

$$\dim(P_{\mathcal{M}(\tilde{G})}) + \dim(P_{\mathcal{M}^*(\tilde{G})}) = |E|,$$

that is, given a graphical matroid, the sum of the dimensions of the OMC polytope of the graphical matroid and the OMC polytope of its dual is equal to the ambient dimension. However, as we can see in the following example this does not hold for any oriented matroid.

Example 2.9. Consider the matrix

$$M = \begin{pmatrix} 1 & 0 & 0 & 1 & 1 & 1 & 1 & 0 & 0 \\ 0 & 1 & 0 & 1 & -1 & 0 & 0 & 1 & 1 \\ 0 & 0 & 1 & 0 & 0 & 1 & -1 & 1 & -1 \end{pmatrix}.$$

whose columns are the type \mathcal{B}_3 positive roots. The oriented matroid $\mathcal{M}(\mathcal{B}_3^+)$ corresponding to the matrix M is not a graphical matroid, and $\dim(P_{\mathcal{M}(\mathcal{B}_3^+)}) = 9$, which is the dimension of the ambient space. Consider, then, the dual oriented matroid. It turns out that $P_{\mathcal{M}^*(\mathcal{B}_3^+)}$ is not a 0-dimensional polytope; in fact, using a computer, we determined that $\dim(P_{\mathcal{M}^*(\mathcal{B}_3^+)}) = 9$ as well.

2.4 Bridges and loops

In Section 3, we carefully study the oriented matroid cocircuit polytope whose underlying matroid is the complete graph on n nodes, K_n . We do not study other OMC polytopes in such detail, but we can make some slightly more general comments.

Proposition 2.10. *Let $\tilde{G} = (V, E)$ be a directed graph with at least one bridge $b \in E$. Then $P_{\mathcal{M}^*(\tilde{G})}$ is a suspension of $P_{\mathcal{M}^*(\tilde{G} \setminus \{b\})}$.*

Proof. Since a bridge is an edge whose removal increases the number of connected components by one, b precisely defines a minimal cut of \tilde{G} . Thus b yields cocircuits of the form $\tilde{X} = (0, \dots, 0, +, 0, \dots, 0)$ and $-\tilde{X} = (0, \dots, 0, -, 0, \dots, 0)$. By circuit axiom (C2), there can be no other circuits of $\mathcal{M}^*(\tilde{G})$ containing \tilde{X} , so every other circuit of $\mathcal{M}^*(\tilde{G})$ comes from a circuit of $\mathcal{M}^*(\tilde{G} \setminus \{b\})$, with a 0 in the spot corresponding to edge b . In particular, $P_{\mathcal{M}^*(\tilde{G})}$ is a suspension of $P_{\mathcal{M}^*(\tilde{G} \setminus \{b\})}$. \square

Consider another special kind of edge: a directed loop. For example, let \tilde{G} be the directed graph that is a set of three directed loops on one node. Every loop contributes two circuits: one from traversing the loop in a positive direction, and the other from traversing the loop in a negative direction. The circuits, then, are $(1, \emptyset)$, $(\emptyset, 1)$, $(2, \emptyset)$, $(\emptyset, 2)$, $(3, \emptyset)$, $(\emptyset, 3)$. Then $P_{\mathcal{M}(\tilde{G})}$ has vertices $(1, 0, 0)$, $(-1, 0, 0)$, $(0, 1, 0)$, $(0, -1, 0)$, $(0, 0, 1)$, $(0, 0, -1)$: it is the three-dimensional cross-polytope. Extending this idea gives us the following proposition.

Proposition 2.11. *Let $\tilde{B} = (V, E)$ be a bouquet, that is, a graph with $|E|$ directed loops. Then $P_{\mathcal{M}(\tilde{B})}$ is the $|E|$ -dimensional cross polytope.*

3 A closer look: The complete graph

Given the complete graph on n nodes K_n , orient the edges (i, j) with $i < j$. Observe that the incidence matrix of this directed graph is the matrix whose columns are the positive roots of A_{n-1} , that is, $e_i - e_j$ with $1 \leq i < j \leq n$. Since the oriented matroid for this directed graph is represented by this matrix, we denote this matroid by \mathcal{A}_{n-1} and its dual by \mathcal{A}_{n-1}^* . In this section we focus on the polytope $P_{\mathcal{A}_{n-1}^*} \subseteq \mathbb{R}^{\binom{n}{2}}$, which we denote by \mathcal{P}_{n-1} to simplify notation. The polytope \mathcal{P}_{n-1} appears in several other contexts, which we use to determine the structure, Ehrhart theory, and even equivariant Ehrhart theory of \mathcal{P}_{n-1} with respect to the previously mentioned S_n action. We also describe this polytope and the fixed polytopes under this action.

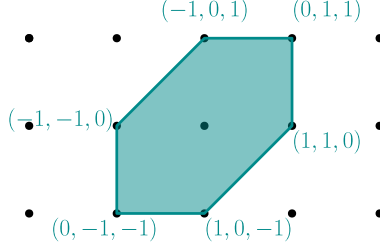


Figure 3: \mathcal{P}_2 with $\text{aff}(\mathcal{P}_2)$ pictured as generated by $(1, 1, 0)$ and $(-1, 0, 1)$.

3.1 The polytope \mathcal{P}_{n-1}

Let \widetilde{K}_n be the complete graph on n nodes, oriented so that each edge is directed from the smaller vertex to the larger vertex. Note that by Remark 2.3, reversing the orientations of some of the edges would yield an isomorphic polytope. By Proposition 2.4, we have that each vertex of \mathcal{P}_{n-1} corresponds with a minimal cut $[n] = V_1 \sqcup V_2$ of K_n . In fact, any partition $[n] = V_1 \sqcup V_2$ with $V_1, V_2 \neq \emptyset$ is a minimal cut of K_n . Throughout this section we denote by $\widehat{\mathbf{u}}_{a_1 \dots a_m}$ the vertex of \mathcal{P}_{n-1} corresponding to the minimal cut with $V_1 = \{a_1, \dots, a_m\}$. In particular, the vertices $\widehat{\mathbf{u}}_I$ of \mathcal{P}_{n-1} are in bijection with subsets $\emptyset \subsetneq I \subsetneq [n]$.

The following corollary is an immediate consequence of Proposition 2.8.

Corollary 3.1. *The dimension of \mathcal{P}_{n-1} is $n - 1$.*

We write the coordinates of $\mathbb{R}^{\binom{n}{2}}$ as x_{ij} for $1 \leq i < j \leq n$, where x_{ij} corresponds to the edge (i, j) of K_n . Note then that given $V_1 = \{a_1, \dots, a_m\}$,

$$(\widehat{\mathbf{u}}_{a_1 \dots a_m})_{ij} := \begin{cases} 1, & i \in V_1, j \in V_2 \\ -1, & i \in V_2, j \in V_1 \\ 0, & \text{otherwise} \end{cases}$$

It is straightforward to check that given $1 \leq i < j \leq n$, every vertex of \mathcal{P}_{n-1} satisfies $x_{ij} - x_{in} + x_{jn} = 0$. Thus, \mathcal{P}_{n-1} is contained in the linear subspace of $\mathbb{R}^{\binom{n}{2}}$ given by the intersection of the $\binom{n-1}{2}$ hyperplanes of the form $x_{ij} - x_{in} + x_{jn} = 0$. These hyperplanes correspond to the cycles of K_n of the form ijn . The reader can confirm that this intersection is $(n - 1)$ -dimensional. Thus, it follows from Corollary 3.1 that this linear subspace is the affine span $\text{aff}(\mathcal{P}_{n-1})$ of \mathcal{P}_{n-1} .

In order to better understand the structure of \mathcal{P}_{n-1} , we discuss zonotopes. For a finite set of vectors $\mathbf{V} = \{\mathbf{v}_1, \dots, \mathbf{v}_n\} \subset \mathbb{R}^d$ we define the **zonotope** of \mathbf{V} to be

$$\mathcal{Z}(\mathbf{V}) := \sum_{i=1}^n [\mathbf{0}, \mathbf{v}_i] := \{\lambda_1 \mathbf{v}_1 + \dots + \lambda_n \mathbf{v}_n \mid \text{for all } i, 0 \leq \lambda_i \leq 1\},$$

where $[\mathbf{0}, \mathbf{v}_i] = \{\lambda \mathbf{v}_i \mid 0 \leq \lambda \leq 1\}$.

Proposition 3.2. *\mathcal{P}_{n-1} is the zonotope $\mathcal{Z}(\widehat{\mathbf{u}}_1, \widehat{\mathbf{u}}_2, \dots, \widehat{\mathbf{u}}_n)$.*

Proof. First, note that (2.1) implies that $\widehat{\mathbf{u}}_{a_1 \dots a_m} = \sum_{i=1}^m \widehat{\mathbf{u}}_{a_i}$ for each $\{a_1, \dots, a_m\} \neq \emptyset, [n]$. Thus, each vertex of \mathcal{P}_{n-1} is in $\mathcal{Z}(\widehat{\mathbf{u}}_1, \widehat{\mathbf{u}}_2, \dots, \widehat{\mathbf{u}}_n)$, i.e. $\mathcal{P}_{n-1} \subseteq \mathcal{Z}(\widehat{\mathbf{u}}_1, \widehat{\mathbf{u}}_2, \dots, \widehat{\mathbf{u}}_n)$. To prove the opposite containment it suffices to verify that each sum $\lambda_1 \widehat{\mathbf{u}}_1 + \dots + \lambda_n \widehat{\mathbf{u}}_n$ with $\lambda_i \in \{0, 1\}$ is in \mathcal{P}_{n-1} . The case in which $\lambda_i = 0$ and $\lambda_j = 1$ for some i, j follows from the equation above. Since $\mathbf{0} \in \mathcal{P}_{n-1}$, the case in which all $\lambda_i = 0$ also follows. For the case in which all $\lambda_i = 1$, note that for any edge e

$$(\widehat{\mathbf{u}}_1)_e + \dots + (\widehat{\mathbf{u}}_n)_e = 1 - 1 = 0$$

and therefore $\widehat{\mathbf{u}}_1 + \dots + \widehat{\mathbf{u}}_n = \mathbf{0} \in \mathcal{P}_{n-1}$. □

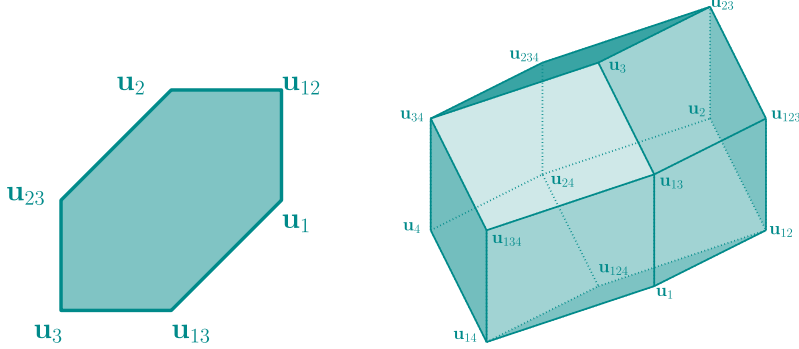


Figure 4: \mathcal{P}_2 (left) and \mathcal{P}_3 (right).

Remark 3.3. One could ask if all graphical matroids yield OMC polytopes that are zonotopes, but it is not the case. Consider, for instance, the graph G which is \widetilde{K}_4 with the edge $\overline{14}$ removed. One can observe that the corresponding cocircuit polytope $P_{\mathcal{M}^*(G)}$ is a 3-dimensional polytope with 14 faces, 8 of which are triangles. Since the faces of a zonotope are also zonotopes but a triangle is not a zonotope, $P_{\mathcal{M}^*(G)}$ is not a zonotope.

It is often easier to work with full-dimensional objects; since \mathcal{P}_{n-1} is an $(n-1)$ -dimensional polytope, we want to view \mathcal{P}_{n-1} as a polytope in \mathbb{R}^{n-1} . We use the projection in which we keep the x_{in} coordinates for $i \in [n-1]$. Since each coordinate is of the form x_{in} for a fixed n , we now write the coordinates as x_i for $i \in [n-1]$. In particular, the projection $\pi : \mathbb{R}^{\binom{n}{2}} \rightarrow \mathbb{R}^{n-1}$ comes from the $(n-1) \times \binom{n}{2}$ matrix

$$(\pi_{ij}) = \begin{cases} 1 & \text{if } j = in - \binom{i+1}{2} \\ 0 & \text{otherwise} \end{cases}$$

and $\pi(\mathcal{P}_{n-1}) = \mathcal{Z}(\mathbf{e}_1, \dots, \mathbf{e}_{n-1}, -\mathbf{1})$, where $\{\mathbf{e}_1, \dots, \mathbf{e}_{n-1}\}$ is the standard basis for \mathbb{R}^{n-1} and $\mathbf{1} := \mathbf{e}_1 + \dots + \mathbf{e}_{n-1}$. For $\emptyset \subsetneq I \subsetneq [n]$, we define $\mathbf{u}_I := \pi(\widehat{\mathbf{u}}_I)$.

Not only is $\pi(\mathcal{P}_{n-1})$ linearly isomorphic to \mathcal{P}_{n-1} , but the two polytopes have the same lattice point count. To verify this, first observe that if $p \in \mathbb{Z}^{\binom{n}{2}}$, it immediately follows that $\pi(p) \in \pi\left(\mathbb{Z}^{\binom{n}{2}}\right)$. On the other hand, consider $p \in \pi\left(\mathbb{Z}^{\binom{n}{2}}\right)$, so $p = (a_1, a_2, \dots, a_{n-1})$ where $a_i \in \mathbb{Z}$. To construct $\pi^{-1}(p) = (a_{12}, a_{13}, \dots, a_{n-1}, n)$, we must have $a_{in} = a_i$. We can then use the equations of the hyperplanes $x_{ij} - x_{in} + x_{jn} = 0$ to ensure that we end up with a point in $\mathbb{Z}^{\binom{n}{2}} \cap \text{aff}(\mathcal{P}_{n-1})$. This tells us that $a_{ij} = a_{in} - a_{jn} = a_i - a_j$. Then $a_i, a_j \in \mathbb{Z}$ implies that $a_{ij} \in \mathbb{Z}$ as well. Thus $\pi^{-1}(p) \in \mathbb{Z} \cap \text{aff}(\mathcal{P}_{n-1})$.

3.2 Other appearances

In addition to being an OMC polytope, \mathcal{P}_{n-1} is found in other, well-studied families of polytopes, in particular, graphic zonotopes and the polar duals of symmetric edge polytopes. Moreover, \mathcal{P}_{n-1} appears in Stapledon's [17] in Example 8.7 and Remark 9.4; we shall return to this last appearance in more detail in Section 3.5.

First, we verify that \mathcal{P}_{n-1} is affinely isomorphic to the graphic zonotope of the cycle with n vertices, denoted C_n . The **graphic zonotope** \mathcal{Z}_G associated to a graph $G = ([n], E)$ is

$$\mathcal{Z}_G := \sum_{\{u,v\} \in E} [\mathbf{e}_u, \mathbf{e}_v].$$

Proposition 3.4. Consider the affine map $\phi : \mathbb{R}^{n-1} \rightarrow \mathbb{R}^n$ given by

$$\phi(\mathbf{x}) := (-x_1 + 1, x_1 - x_2 + 1, \dots, x_{n-2} - x_{n-1} + 1, x_{n-1} + 1).$$

We have that $\phi(\mathcal{Z}(\mathbf{e}_1, \dots, \mathbf{e}_{n-1}, -\mathbf{1})) = \mathcal{Z}_{C_n}$ and thus \mathcal{P}_{n-1} is affinely isomorphic to \mathcal{Z}_{C_n} .

Proof. Fix $\mathbf{v} = \lambda_1 \mathbf{e}_1 + \dots + \lambda_{n-1} \mathbf{e}_{n-1} - \lambda_n \mathbf{1} = (\lambda_1 - \lambda_n, \dots, \lambda_{n-1} - \lambda_n) \in \mathcal{Z}(\mathbf{e}_1, \dots, \mathbf{e}_{n-1}, -\mathbf{1})$ so that $\lambda_i \in [0, 1]$ for all i . Direct computation shows that

$$\begin{aligned} \phi(\mathbf{v}) &= (1 - \lambda_1 + \lambda_n, \lambda_1 + 1 - \lambda_2, \dots, \lambda_{n-2} + 1 - \lambda_{n-1}, \lambda_{n-1} + 1 - \lambda_n) \\ &= ((1 - \lambda_1)\mathbf{e}_1 + \lambda_1 \mathbf{e}_2) + \dots + ((1 - \lambda_{n-1})\mathbf{e}_{n-1} + \lambda_{n-1} \mathbf{e}_n) + ((1 - \lambda_n)\mathbf{e}_n + \lambda_n \mathbf{e}_1) \end{aligned} \quad (3.1)$$

and the last expression shows that $\phi(\mathbf{v}) \in \mathcal{Z}_{C_n}$. The opposite containment also follows from Equation (3.1). \square

Given a graph G with node set $V = [n]$, the **symmetric edge polytope** (SEP) associated to G is the polytope

$$\mathcal{S}_G := \text{conv}\{\pm(\mathbf{e}_i - \mathbf{e}_j) \mid \{i, j\} \in E(G)\}.$$

Symmetric edge polytopes themselves are quite interesting (see, for example, [13, Section 6.1]) and sometimes make an appearance in other contexts (see, for instance, [7, Section 2]). When G is the complete graph K_n on n nodes, \mathcal{S}_{K_n} is the root polytope of the lattice A_n .

The polar duals of symmetric edge polytopes are also of interest [8]. Let P be a d -dimensional lattice polytope containing the origin in its interior. The **polar dual** of P is the polytope

$$P^\vee := \{\mathbf{u} \in \mathbb{R}^d \mid \mathbf{u} \cdot \mathbf{x} \leq 1 \text{ for every } \mathbf{x} \in P\}.$$

When P^\vee is a lattice polytope, we say that P is **reflexive**. Symmetric edge polytopes are known to be reflexive. We find a connection to OMC polytopes: the polar dual of the SEP \mathcal{S}_{K_n} is the tropical unit ball, defined in [6, Section 2] and further investigation shows that, in fact, \mathcal{P}_{n-1} is a tropical unit ball. Concretely, $\mathcal{P}_{n-1} = \mathcal{S}_{K_n}^\vee$. One could ask if this relation between SEPs and OMC polytopes holds for all graphs, but this is not the case.

Consider, for example, the graph $G = K_4 \setminus e$, where e is the edge 24, and let \tilde{G} be the directed graph obtained by orienting the edges of G as $\vec{12}$, $\vec{23}$, $\vec{34}$, $\vec{41}$, and $\vec{13}$. The polar dual of the SEP of \tilde{G} is given in [8, Example 5.2]. The polytopes $\mathcal{S}_{\tilde{G}}$ and $P_{\mathcal{M}^*(\tilde{G})}$, pictured in Figure 5, are distinct polytopes. In particular,

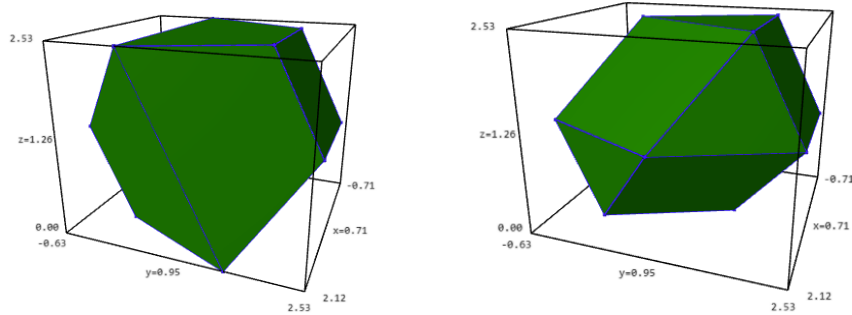


Figure 5: The polar dual of the symmetric edge polytope $\mathcal{S}_{\tilde{G}}$ (left) and the OMC polytope $P_{\mathcal{M}^*(\tilde{G})}$ (right).

one can see that the facets of $\mathcal{S}_{\tilde{G}}$ are all quadrilaterals, whereas the facets of $P_{\mathcal{M}^*(\tilde{G})}$ are both quadrilaterals and triangles.

3.3 Face structure of \mathcal{P}_{n-1}

Next, we study the face structure of \mathcal{P}_{n-1} . In [1, Lemma 13.4], a concrete bijection is given between the proper faces of a graphic zonotope \mathcal{Z}_G and the pairs (f, \mathcal{O}) , where $f \subset E$ is a flat of the graph G and \mathcal{O} is an acyclic orientation of the contraction G/f . To construct the face corresponding to (f, \mathcal{O}) , one first constructs the graph $g(f, \mathcal{O})$ obtained from G by fixing the edges in f and replacing each edge $\{v, w\} \notin f$ with the half-edge $\{v\}$, where $v \rightarrow w$ in \mathcal{O} . The face corresponding to (f, \mathcal{O}) is the zonotope

$$\mathcal{Z}_{g(f, \mathcal{O})} = \sum_{\substack{\{v_j\} \text{ is a halfedge} \\ \text{of } g(f, \mathcal{O})}} \Delta_j + \sum_{\substack{e_j \text{ is an edge} \\ \text{of } g(f, \mathcal{O})}} \Delta_{j, j+1},$$

where $\Delta_j = \mathbf{e}_j$ and $\Delta_{j, j+1} = [\mathbf{e}_j, \mathbf{e}_{j+1}]$. In the following theorem, we use this description in the case $G = C_n$ to describe the faces of \mathcal{P}_{n-1} .

Theorem 3.5. *For $0 \leq i < n - 1$, the following is a bijection*

$$\begin{aligned} \{(S, T) : \emptyset \subsetneq S \subseteq T \subsetneq [n], |T \setminus S| = i\} &\rightarrow \{i\text{-dimensional faces of } \mathcal{P}_{n-1}\} \\ (S, T) &\mapsto \sum_{j \in S} \mathbf{u}_j + \sum_{j \in T \setminus S} [\mathbf{0}, \mathbf{u}_j]. \end{aligned}$$

Proof. To show the desired bijection, we use the fact that \mathcal{P}_{n-1} is affinely isomorphic to the graphic zonotope \mathcal{Z}_{C_n} . We first identify a bijection between the set of pairs (S, T) and the set of pairs (f, \mathcal{O}) . Then, we compose this bijection with the map ϕ in Proposition 3.4.

Start with a planar realization of C_n . Throughout this proof, our labels are integers modulo n ; in particular, $n + 1 = 1$. Denote by v_1, \dots, v_n the vertices of C_n , oriented so that the labels increase clockwise, and let $e_j \in E$ denote the edge $\{v_j, v_{j+1}\}$. Let $f_I = \{e_j \mid j \in I\}$. Then the flats of C_n are f_I for $I = [n]$ and $I \in \binom{[n]}{k}$ for $k = 0, \dots, n - 2$. Since we are interested in proper faces and the face of the polytope corresponding to $I = [n]$ is the polytope itself, we exclude this case.

Consider the pair (S, T) and the flat $f = f_{T \setminus S}$. We construct the following orientation \mathcal{O} from S , assigning each edge $e_j \in C_n/f$ the orientation \mathcal{O}_j :

$$\mathcal{O}_j = \begin{cases} \text{counterclockwise,} & j \in S \\ \text{clockwise,} & j \notin S. \end{cases} \quad (3.2)$$

This map is surjective: consider a flat and orientation pair (f, \mathcal{O}) . Then

$$\begin{aligned} S &= \{j \in [n] \mid e_j \text{ has a counterclockwise orientation in } \mathcal{O}\} \\ T &= S \cup \{j \in [n] \mid e_j \in f\}. \end{aligned}$$

Observe that $S \neq \emptyset$ since $S = \emptyset$ would yield an all-clockwise orientation and that $T \neq [n]$ since $T = [n]$ would yield an all-counterclockwise orientation, neither of which are acyclic.

To see that we have a bijection, we compare the cardinality of both sets.

For $\{(S, T) \mid \emptyset \subsetneq S \subseteq T \subsetneq [n]\}$, since $S \neq \emptyset$ and $T \neq [n]$, $T \setminus S$ can have size $k = 0, \dots, n - 2$, and for each value of k , there are $\binom{n}{k}$ possible choices for elements of $T \setminus S$. Now, given $T \setminus S$ with $|T \setminus S| = k$, we examine the remaining $n - k$ elements of $[n]$. Each element can either be in S or not, giving 2^{n-k} total options. However, since $S \neq \emptyset$ and $T \neq [n]$, we subtract two of those options. Thus the cardinality is $\sum_{k=0}^{n-2} \binom{n}{k} (2^{n-k} - 2)$.

For $\{(f, \mathcal{O}) \mid f \neq E \text{ flat of } C_n, \mathcal{O} \text{ acyclic orientation of } C_n/f\}$, we obtain a flat f_I for each $I \in \binom{[n]}{k}$ for $k = 0, \dots, n - 2$. For each flat f_I with $|I| = k$, we need to count the acyclic orientations of C_n/f_I . C_n/f_I is now another cycle graph, with $n - k$ edges. The only orientations that are not acyclic are the all-clockwise

and all-counterclockwise orientations. Thus overall we obtain $2^{n-k} - 2$ acyclic orientations. Putting this all together, the cardinality is $\sum_{k=0}^{n-2} \binom{n}{k} (2^{n-k} - 2)$, as desired.

Thus we have a bijection

$$\{(S, T) \mid \emptyset \subsetneq S \subseteq T \subsetneq [n]\} \leftrightarrow \{(f, \mathcal{O}) \mid f \neq E \text{ flat of } C_n, \mathcal{O} \text{ acyclic orientation of } C_n/f\}.$$

We next want to relate the elements (f, \mathcal{O}) with proper faces of \mathcal{Z}_{C_n} . Applying [1, Lemma 13.4] and the above bijection, we get

$$\begin{aligned} \mathcal{Z}_{g(f_{T \setminus S}, \mathcal{O})} &= \sum_{\substack{\{v_j\} \text{ is a halfedge} \\ \text{of } g(f_{T \setminus S}, \mathcal{O})}} \Delta_j + \sum_{\substack{e_j \text{ is an edge} \\ \text{of } g(f_{T \setminus S}, \mathcal{O})}} \Delta_{j, j+1} \\ &= \sum_{j \in T \setminus S} \Delta_{j, j+1} + \sum_{j \in S} \Delta_{j+1} + \sum_{j \notin T} \Delta_j, \end{aligned}$$

where $\Delta_j = \mathbf{e}_j$ and $\Delta_{j, j+1} = [\mathbf{e}_j, \mathbf{e}_{j+1}]$. Our final step, then, is to determine which faces of \mathcal{P}_{n-1} correspond to each $\mathcal{Z}_{g(f, \mathcal{O})}$. Towards this step, consider the map $\phi : \mathcal{P}_{n-1} \rightarrow \mathcal{Z}_{C_n}$ given in Proposition 3.4. We claim that

$$\sum_{j \in S} \mathbf{u}_j + \sum_{j \in T \setminus S} [0, \mathbf{u}_j] \mapsto \mathcal{Z}_{g(f_{T \setminus S}, \mathcal{O})},$$

where \mathcal{O} is the orientation defined in (3.2).

Let $\mathbf{v} \in \sum_{j \in S} \mathbf{u}_j + \sum_{j \in T \setminus S} [0, \mathbf{u}_j]$. To determine $\phi(\mathbf{v})$, we rewrite \mathbf{v} as a single sum:

$$\begin{aligned} \mathbf{v} &= \sum_{j \in S} \mathbf{u}_j + \sum_{j \in T \setminus S} \lambda_j \mathbf{u}_j, & \lambda_j &\in [0, 1] \text{ for } j \in T \setminus S \\ &= \sum_{j \in [n]} \lambda_j \mathbf{u}_j, & \lambda_j &= \begin{cases} 1, & j \in S \\ 0, & j \notin T \\ x \in [0, 1], & j \in T \setminus S. \end{cases} \end{aligned}$$

Then, by the proof of Proposition 3.4,

$$\phi(\mathbf{v}) = ((1 - \lambda_1)\mathbf{e}_1 + \lambda_1\mathbf{e}_2) + \cdots + ((1 - \lambda_{n-1})\mathbf{e}_{n-1} + \lambda_{n-1}\mathbf{e}_n) + ((1 - \lambda_n)\mathbf{e}_n + \lambda_n\mathbf{e}_1).$$

Now, we can consider each of the three cases:

1. If $j \in S$, then $\lambda_j = 1$, so $(1 - \lambda_j)\mathbf{e}_j + \lambda_j\mathbf{e}_{j+1} = \mathbf{e}_{j+1} = \Delta_{j+1}$.
2. If $j \notin T$, then $\lambda_j = 0$, so $(1 - \lambda_j)\mathbf{e}_j + \lambda_j\mathbf{e}_{j+1} = \mathbf{e}_j = \Delta_j$.
3. If $j \in T \setminus S$, then $\lambda_j \in [0, 1]$, so $(1 - \lambda_j)\mathbf{e}_j + \lambda_j\mathbf{e}_{j+1} \in \Delta_{j, j+1}$.

Thus $\phi(\mathbf{v}) \in \mathcal{Z}_{g(f_{T \setminus S}, \mathcal{O})}$ as desired. Moreover, varying λ_j in the third case yields the whole interval $\Delta_{j, j+1}$, and thus this map is surjective. \square

The following follows from the description of the face corresponding to (S, T) in the preceding theorem.

Corollary 3.6. *The face lattice of \mathcal{P}_{n-1} is isomorphic to the poset $(\{(S, T) : \emptyset \subsetneq S \subseteq T \subsetneq [n]\}, \preceq)$, where $(S_1, T_1) \preceq (S_2, T_2)$ if and only if $T_1 \subseteq T_2$ and $S_2 \subseteq S_1$.*

Given a d -dimensional polytope \mathcal{P} and $0 \leq i \leq d$, let $f_i(\mathcal{P})$ denote the number of i -dimensional faces of \mathcal{P} . The f -polynomial of \mathcal{P} is then $f_{\mathcal{P}}(t) := \sum_{i=0}^d f_i(\mathcal{P}) t^i$. Using the theorem above, we immediately obtain the f -polynomial of \mathcal{P}_{n-1} , which due to Proposition 3.4 recovers a formula by Grujić.

Corollary 3.7. [14, Proposition 5.2] *The f -polynomial of \mathcal{P}_{n-1} is $f_{\mathcal{P}_{n-1}}(t) = t^{n-1} + \sum_{i=0}^{n-2} (2^{n-i} - 2) \binom{n}{i} t^i$.*

3.4 Ehrhart theory of \mathcal{P}_{n-1}

We now introduce Ehrhart theory. The **lattice point enumerator** of a polytope P is

$$L_P(t) := \#(tP \cap \mathbb{Z}^d).$$

Theorem 3.8. [11] *Let P be an integral convex d -polytope; then $L_P(t)$ is a polynomial in t of degree d with leading term $\text{vol}(P)$ and constant term 1.*

When P is integral, we call $L_P(t)$ the **Ehrhart polynomial** of P and sometimes denote it $\text{ehr}_P(t)$ instead of $L_P(t)$. The generating function of $L_P(t)$ is called the **Ehrhart series** of $L_P(t)$ and is denoted $\text{Ehr}_P(z)$:

$$\text{Ehr}_P(z) := 1 + \sum_{t \geq 1} L_P(t) z^t = \frac{h_d^* z^d + h_{d-1}^* z^{d-1} + \cdots + h_1^* z + h_0^*}{(1-z)^{d+1}}.$$

The numerator polynomial $h_P^*(z)$ is called the **h^* -polynomial** of P , and when written in vector form, it is called the **h^* -vector**: $h^*(P) := (h_0^*, \dots, h_d^*)$.

Next, we describe the Ehrhart polynomial and series of \mathcal{P}_{n-1} . Since Eulerian polynomials will play a role, we proceed to introduce them. For a positive integer n , the **Eulerian polynomial** is $A_n(t) = \sum_{i=0}^{n-1} A(n, i) t^i$, where the **Eulerian number** $A(n, i)$ is the number of permutations in S_n with exactly i descents. The Ehrhart theory of \mathcal{P}_{n-1} follows as a corollary of [16, Exercise 4.64b].

Proposition 3.9. *The Ehrhart polynomial of \mathcal{P}_{n-1} is*

$$\text{ehr}_{\mathcal{P}_{n-1}}(t) = (t+1)^n - t^n = \sum_{k=0}^{n-1} \binom{n}{k} t^k.$$

The Ehrhart series of \mathcal{P}_{n-1} is

$$\text{Ehr}_{\mathcal{P}_{n-1}}(z) = \frac{A_n(z)}{(1-z)^n}.$$

Proof. We apply Stanley's method for computing the Ehrhart polynomial of graphic zonotopes [16, Exercise 4.64b]. Since $\mathcal{P}_{n-1} \cong \mathcal{Z}_{C_n}$, we need to count the number of subtrees of C_n with j edges to obtain the coefficient of t^k in $\text{ehr}_{\mathcal{P}_{n-1}}(t)$. Since C_n is itself just a cycle, any subset of $k \neq n$ edges forms a tree. In particular, the coefficient of t^k is $\binom{n}{k}$ for $0 \leq k \leq n-1$.

Then the Ehrhart series is

$$\begin{aligned} \text{Ehr}_{\mathcal{P}_{n-1}}(z) &= 1 + \sum_{t \geq 1} ((t+1)^n - t^n) z^t \\ &= \sum_{t \geq 0} (t+1)^n z^t - \sum_{t \geq 1} t^n z^t \\ &= \sum_{t \geq 1} \frac{t^n}{z} z^t - \sum_{t \geq 1} t^n z^t \\ &= \left(\frac{1-z}{z} \right) \sum_{t \geq 1} t^n z^t \\ &= (1-z) \frac{\sum_{k=1}^n A(n, k) z^{k-1}}{(1-z)^{n+1}} \\ &= \frac{A_n(z)}{(1-z)^n}, \end{aligned}$$

where the last equation follows from a well known identity of the Eulerian polynomial, see e.g. [16, Proposition 1.4.4].¹ \square

We remark that the h^* -polynomial of \mathcal{P}_{n-1} is strikingly similar to the h^* -polynomial of the n -dimensional unit cube \square_n , which is

$$\text{Ehr}_{\square_n}(z) = \frac{A_n(z)}{(1-z)^{n+1}}.$$

3.5 Equivariant Ehrhart theory of \mathcal{P}_{n-1}

We begin by introducing equivariant Ehrhart theory for general polytopes. The polytopes we are examining are all full-dimensional, and thus their affine spans contain the origin, so we will focus on that specific case; for the more general construction, see Stapledon [17]. Let $P \subset \mathbb{R}^n$ be a n -dimensional lattice polytope and G be a group that acts linearly on \mathbb{Z}^n and such that P is invariant under the action of G . Let \mathbf{M} be the intersection of \mathbb{Z}^n with the linear span of P . Now \mathbf{M} is G -invariant, and we obtain a representation $\rho : G \rightarrow GL(\mathbf{M})$.

Let χ_{tP} denote the permutation character associated to the action of G on the lattice points in the t th dilate of P . Given $g \in G$, let

$$P^g = \{p \in P \mid g \cdot p = p\},$$

that is, P^g is the polytope of points $p \in P$ fixed by g . In [17, Lemma 5.2] it is shown that $\chi_{tP}(g) = L_{P^g}(t)$.

Consider the function $H^* : G \rightarrow \mathbb{Z}[[z]]$ given by

$$H^*[z](g) := (1-z) \det(I - g \cdot z) \sum_{t \geq 0} \chi_{tP}(g) z^t,$$

called the **equivariant H^* -series** of P . If we rearrange the above equation to isolate the sum, we obtain something that looks like an Ehrhart series; indeed, when we consider the identity element $e \in G$, $H^*[z](e)$ is in fact the h^* -polynomial of P .

We now describe the linear S_n -action on \mathcal{P}_{n-1} with respect to which we will compute the Equivariant Ehrhart Theory. Stapledon [17] uses a connection with the cohomology of the toric variety of the permutahedron and previous computations of Stembridge [18] to compute the equivariant Ehrhart theory of \mathcal{P}_{n-1} , and therefore shows that \mathcal{P}_{n-1} satisfies [17, Conjecture 12.1]. We do so directly using the fixed polytopes. Given $\sigma \in S_n$, we describe this action using the $(n-1) \times (n-1)$ matrix M_σ , defined by

$$((M_\sigma)_{ij}) = \begin{cases} 1 & \text{if } \sigma(j) = i, \\ -1 & \text{if } \sigma(j) = n, \\ 0 & \text{otherwise.} \end{cases}$$

Note that for a vertex $\mathbf{u}_{a_1 \dots a_m}$ of \mathcal{P}_{n-1} ,

$$M_\sigma \cdot \mathbf{u}_{a_1 \dots a_m} = \mathbf{u}_{\sigma(a_1) \dots \sigma(a_m)},$$

that is, the S_n action applied to a vertex can be described as $\sigma \in S_n$ shuffling the elements of the set labeling that vertex. For example, the transposition (23) in \mathcal{P}_2 fixes the vertices \mathbf{u}_1 and \mathbf{u}_{23} , switches \mathbf{u}_2 and \mathbf{u}_3 , and switches \mathbf{u}_{12} and \mathbf{u}_{13} . One can verify using $M_{(23)}$ that $\mathcal{P}_2^{(23)}$ is a line segment, as shown in Figure 6.

By definition, if $M_\sigma \cdot \mathbf{u}_I = \mathbf{u}_J$, then I and J have the same size. Moreover, given $I = \{a_1, \dots, a_m\}$ and $J = \{b_1, \dots, b_m\}$, there exists a permutation σ , for instance, $\sigma = (a_1 b_1) \cdots (a_m b_m)$, that sends \mathbf{u}_I to \mathbf{u}_J . Thus the orbits of this S_n action are of the form $\{\mathbf{u}_I \mid |I| = m\}$ for each $1 \leq m < n$.

We next compute the polynomial $H^*[z](\sigma)$. Let $\sigma \in S_n$ have cycle decomposition $\sigma = \alpha_1 \cdots \alpha_k$, where α_k contains n . Let $\tilde{\alpha}_i$ be the set of elements of $[n]$ permuted by the cycle α_i .

¹We warn the reader that the conventions in [16] for Eulerian polynomials differ from ours by a factor of t .

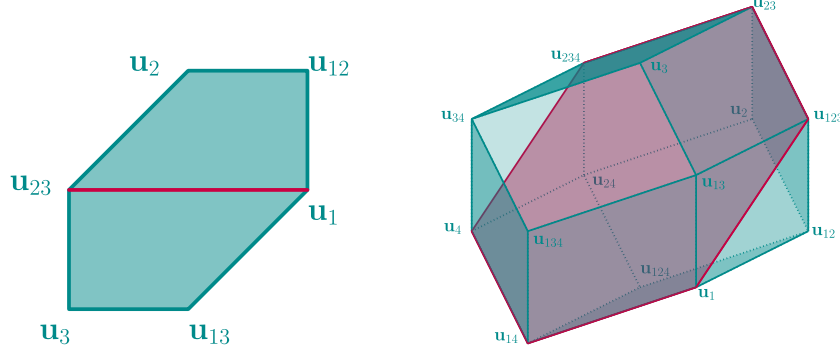


Figure 6: The fixed polytopes $\mathcal{P}_2^{(23)}$ and $\mathcal{P}_3^{(23)}$.

Remark 3.10. The equivariant Ehrhart theory of graphic zonotopes is computed in [12]. While \mathcal{P}_{n-1} is a graphic zonotope, the action we describe is different than the action described in [12]. We expand on this in Section 3.6.

Theorem 3.11. Let \mathcal{P}_{n-1}^σ be the fixed polytope of $\sigma \in S_n$, where σ has cycle decomposition $\sigma = \alpha_1 \cdots \alpha_k$. Then $\mathcal{P}_{n-1}^\sigma = \mathcal{Z}(\mathbf{u}_{\tilde{\alpha}_1}, \dots, \mathbf{u}_{\tilde{\alpha}_k})$. As a consequence, its Ehrhart polynomial is

$$L_{\mathcal{P}_{n-1}^\sigma}(t) = \sum_{j=0}^{k-1} \binom{k}{j} t^j = (t+1)^k - t^k,$$

and its h^* -polynomial is the k th Eulerian polynomial $A_k(z)$.

Proof. Consider vertex \mathbf{u}_I of \mathcal{P}_{n-1} and $\sigma \in S_n$, where σ has cycle decomposition $\sigma = \alpha_1 \cdots \alpha_k$; assume n appears in the cycle α_k . In order to determine if \mathbf{u}_I is fixed by σ , we consider what each cycle does to \mathbf{u}_I .

- If $\tilde{\alpha}_i \subseteq I$, then $\alpha_i(\mathbf{u}_I) = \mathbf{u}_I$ since the elements being permuted are fully contained in I .
- If $\tilde{\alpha}_i \cap I = \emptyset$, then $\alpha_i(\mathbf{u}_I) = \mathbf{u}_I$ since none of the elements being permuted are contained in I .
- If $\tilde{\alpha}_i \cap I \neq \emptyset$ and $\tilde{\alpha}_i \not\subseteq I$, then $\alpha_i(\mathbf{u}_I) \neq \mathbf{u}_I$ since some elements of I will be sent to elements not in I and some elements not in I will be sent to elements in I .

Putting these together, we can see that $\sigma(\mathbf{u}_I) = \mathbf{u}_I$ exactly when for each i , either $\tilde{\alpha}_i \subseteq I$ or $\tilde{\alpha}_i \cap I = \emptyset$. Since $\mathbf{u}_I = \sum_{j \in I} \mathbf{u}_j$, this also tells us that $\mathcal{Z}(\mathbf{u}_{\tilde{\alpha}_1}, \dots, \mathbf{u}_{\tilde{\alpha}_k}) \subseteq \mathcal{P}_{n-1}^\sigma$.

For the opposite containment, observe that \mathcal{P}_{n-1}^σ is contained in the hyperplanes defined, for $i < k$, by $x_a = x_b$ if $a, b \in \tilde{\alpha}_i$, and $x_c = 0$ for $c \in \tilde{\alpha}_k \setminus \{n\}$. To see why $x_c = 0$, we consider two cases. First, assume $|\tilde{\alpha}_k| = 2$ and write $\alpha_k = (jn)$. The j th row of the corresponding matrix M_σ will be $-\mathbf{e}_j$, i.e. all zeroes except a -1 at the j -th entry. Applying M_σ to a point $p = (p_1, \dots, p_{n-1}) \in \mathbb{R}^{n-1}$, then, will map p_j to $-p_j$. In order for p to be fixed by M_σ , it must be that $p_j = 0$.

Suppose, then, that $|\tilde{\alpha}_k| = m > 2$; say $\alpha_k = (a_1 a_2 \dots a_{m-1} n)$. The a_i th column of the corresponding matrix M_σ is $\mathbf{e}_{a_{i+1}}$ and the a_{m-1} st column is $-\mathbf{1}$. Applying M_σ to $p \in \mathbb{R}^{n-1}$ yields

$$\begin{aligned} p_{a_1} &\mapsto -p_{a_{m-1}} \\ p_{a_i} &\mapsto p_{a_{i+1}} - p_{a_{m-1}} \text{ for } i = \{2, \dots, m-1\}. \end{aligned}$$

Solving the system of equations obtained from p being fixed yields $p_{a_i} = 0$ for all $i \in [m-1]$. We conclude that for $p = (p_1, \dots, p_{n-1}) \in \mathcal{P}_{n-1}^\sigma$, $p_a = p_b$ whenever $a, b \in \tilde{\alpha}_i$ for some i . Denote by $p_{\tilde{\alpha}_i}$ the value of p_a for $a \in \tilde{\alpha}_i$.

Now, we need to show that $p = \sum_{i=1}^k \lambda_i \mathbf{u}_{\tilde{\alpha}_i}$ for $0 \leq \lambda_i \leq 1$. Since $p \in \mathcal{P}_{n-1}$, we know that $0 \leq |p_j| \leq 1$ for each j . Next, we know that the sum of the \mathbf{u}_i s is 0; observe, then, since the $\tilde{\alpha}_i$ s form a partition of n , that $\mathbf{u}_{\tilde{\alpha}_k} = -\sum_{i=1}^{k-1} \mathbf{u}_{\tilde{\alpha}_i}$. It is clear that $p = \sum_{i=1}^{k-1} p_{\tilde{\alpha}_i} \mathbf{u}_{\tilde{\alpha}_i}$. If each $p_{\tilde{\alpha}_i} \geq 0$, we are done; suppose, then, that this is not the case. Let $\lambda_k = \max_{i \leq k-1} \{-p_{\tilde{\alpha}_i}\}$ and for $i < k$, let $\lambda_i = p_{\tilde{\alpha}_i} + \lambda_k$. Since $-\lambda_k \leq p_{\tilde{\alpha}_i}$ for each i , $\lambda_i \geq 0$. Moreover, points in \mathcal{P}_{n-1} satisfy $x_j - x_i \leq 1$ and $x_j - x_i \geq -1$, for $i < j$, so $\lambda_i \leq 1$. Then

$$p = \sum_{i=1}^k \lambda_i \mathbf{u}_{\tilde{\alpha}_i}.$$

Hence $\mathcal{P}_{n-1}^\sigma = \mathcal{Z}(\mathbf{u}_{\tilde{\alpha}_1}, \dots, \mathbf{u}_{\tilde{\alpha}_k})$. Moreover, observe that $\mathbf{u}_{\tilde{\alpha}_1}, \dots, \mathbf{u}_{\tilde{\alpha}_{k-1}}$ are linearly independent. Since each $\mathbf{u}_{\tilde{\alpha}_i}$ is a primitive lattice vector and $\mathbf{u}_{\tilde{\alpha}_k} = -\sum_{i=1}^{k-1} \mathbf{u}_{\tilde{\alpha}_i}$, \mathcal{P}_{n-1}^σ is unimodularly equivalent to \mathcal{P}_{k-1} .

The second claim follows from Proposition 3.9. \square

We now prove directly a result that can be recovered from Stapledon's [17, Prop 8.1] and Stembridge's [18, Cor 6.1].

Corollary 3.12. *Let $\sigma \in S_n$ have cycle decomposition $\sigma = \alpha_1 \cdots \alpha_k$. The equivariant H^* -series of \mathcal{P}_{n-1} is given by*

$$H^*[z](\sigma) = A_k(z) \prod_{j=1}^k (1 + z + \cdots + z^{|\tilde{\alpha}_j|-1}).$$

Proof. Let $\sigma \in S_n$. Then

$$\begin{aligned} \det(I - M_\sigma \cdot z) &= \prod_{i=1}^k (1 - z^{|\tilde{\alpha}_i|}) = \prod_{i=1}^k (1 - z) (1 + z + \cdots + z^{|\tilde{\alpha}_i|-1}) \\ &= (1 - z)^k \prod_{i=1}^k (1 + z + \cdots + z^{|\tilde{\alpha}_i|-1}). \end{aligned}$$

Now, we know that the Ehrhart series of \mathcal{P}_{n-1}^σ is

$$\text{Ehr}_{\mathcal{P}_{n-1}^\sigma}(z) = \frac{A_k(z)}{(1 - z)^{k+1}}.$$

Since the denominator of the equivariant Ehrhart series of σ has an extra factor of $1 - z$, the only difference is the product of sums of powers of z . In particular,

$$H^*[z](\sigma) = A_k(z) \prod_{i=1}^k (1 + z + \cdots + z^{|\tilde{\alpha}_i|-1}). \quad \square$$

This equivariant H^* -series shows up elsewhere, for instance in [15, Proposition 6.6], as the Frobenius characteristic of the permutation representation of the toric variety associated to the permutahedron.

3.6 Two equivariant Ehrhart theories

In [12, Section 3.1] the equivariant Ehrhart theory of \mathcal{Z}_{C_n} is studied with respect to a particular group action. The automorphism group of the graph, $\text{Aut}(C_n)$, acts on $[n]$ to shuffle the nodes of the graph while leaving the edge set invariant, which induces a linear action on \mathbb{R}^n under which \mathcal{Z}_{C_n} is invariant. Observe that $\text{Aut}(C_n) \neq S_n$: consider the transposition $\sigma = (23)$ acting on C_4 . Permuting nodes 2 and 3 changes the edge set by replacing edges 12 and 34 with edges 13 and 24, as seen in Figure 7.

Cycle type of $\sigma \in S_4$	$L_{\mathcal{P}_3^\sigma}(t)$	$\sum_{t \geq 0} \chi_{t\mathcal{P}_3}(g)z^t$	$H^*[z](\sigma)$
(1, 1, 1, 1)	$4t^3 + 6t^2 + 4t + 1$	$\frac{(1+11z+11z^2+z^3)(1)}{(1-z)^4}$	$1 + 11z + 11z^2 + z^3$
(2, 1, 1)	$3t^2 + 3t + 1$	$\frac{(1+4z+z^2)(1+z)}{(1-z)(1-z)(1-z^2)}$	$1 + 5z + 5z^2 + z^3$
(2, 2)	$2z + 1$	$\frac{(1+z)(1+z)(1+z)}{(1-z^2)(1-z^2)}$	$1 + 3z + 3z^2 + z^3$
(3, 1)	$2z + 1$	$\frac{(1+z)(1+z+z^2)}{(1-z)(1-z^3)}$	$1 + 2z + 2z^2 + z^3$
(4)	1	$\frac{(1)(1+z+z^2+z^3)}{1-z^4}$	$1 + z + z^2 + z^3$

Table 1: The equivariant H^* -series of \mathcal{P}_3 .

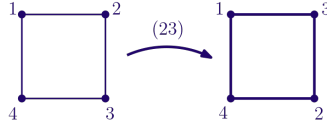


Figure 7: C_4 with (23) applied.



Figure 8: The σ -connectivity graph $C_{C_4}(\sigma)$.

Now, by Proposition 3.4, this action by $\text{Aut}(C_n)$ also gives an equivariant Ehrhart theory for \mathcal{P}_{n-1} . The $\text{Aut}(C_n)$ action is very different from the S_n action we have already studied. As an example, consider $n = 4$ and $\sigma = (24)$. By Theorem 3.11, we know that \mathcal{P}_{4-1}^σ is a hexagon, since $\sigma = (1)(3)(24)$. On the other hand, [12, Theorem 3.11] tells us that the fixed polytope under the $\text{Aut}(C_n)$ action has as many vertices as there are acyclic orientations of the σ -connectivity graph $C_{C_4}(\sigma)$, shown in Figure 8. As there are 4 acyclic orientations of $C_{C_4}(\sigma)$, the corresponding fixed polytope has 4 vertices, not 6. The two different fixed polytopes are shown in Figure 9.

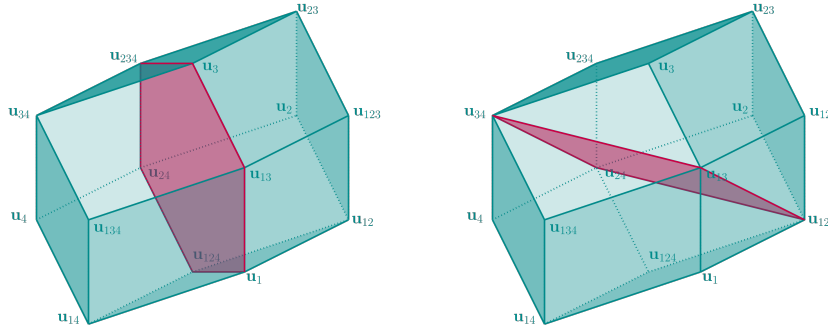


Figure 9: $\mathcal{P}_3^{(24)}$ versus $\mathcal{Z}_{C_4}^{(24)}$.

Acknowledgments

We would like to thank the organizers of the REACT 2021 workshop for organizing the workshop that led us to these polytopes. We are also grateful to Matthias Beck for posing this problem and to Matthias Beck and John Shareshian for many fruitful conversations. Laura Escobar was partially supported by NSF Grant DMS-1855598 and NSF CAREER Grant DMS-2142656. Jodi McWhirter was partially supported by NSF Grant DMS-1855598.

References

- [1] Marcelo Aguiar and Federico Ardila, *Hopf monoids and generalized permutahedra*, Mem. Amer. Math. Soc. **289** (2023), no. 1437, vi+119. [10](#), [11](#)
- [2] Federico Ardila, Anna Schindler, and Andrés R. Vindas-Meléndez, *The equivariant volumes of the permutahedron*, Discrete Comput. Geom. **65** (2021), no. 3, 618–635. MR 4226485 [1](#)
- [3] Federico Ardila, Mariel Supina, and Andrés R. Vindas-Meléndez, *The equivariant Ehrhart theory of the permutahedron*, Proc. Amer. Math. Soc. **148** (2020), no. 12, 5091–5107. [1](#)
- [4] Anders Björner, Michel Las Vergnas, Bernd Sturmfels, Neil White, and Günter M. Ziegler, *Oriented matroids*, second ed., Encyclopedia of Mathematics and its Applications, vol. 46, Cambridge University Press, Cambridge, 1999. [2](#), [3](#), [4](#), [5](#)
- [5] Oliver Clarke, Akihiro Higashitani, and Max Kölbl, *The equivariant Ehrhart theory of polytopes with order-two symmetries*, Proc. Amer. Math. Soc. **151** (2023), no. 9, 4027–4041. [1](#)
- [6] Francisco Criado, Michael Joswig, and Francisco Santos, *Tropical bisectors and Voronoi diagrams*, Found. Comput. Math. **22** (2022), no. 6, 1923–1960. [1](#), [9](#)
- [7] Alessio D’Ali, Emanuele Delucchi, and Mateusz Michałek, *Many faces of symmetric edge polytopes*, Electron. J. Combin. **29** (2022), no. 3, Paper No. 3.24, 42. [9](#)
- [8] Alessio D’Ali, Martina Juhnke-Kubitzke, and Melissa Koch, *On a generalization of symmetric edge polytopes to regular matroids*, International Mathematics Research Notices **2024** (2024), no. 14, 10844–10864. [2](#), [9](#)
- [9] Jesús A. De Loera, David C. Haws, and Matthias Köppe, *Ehrhart polynomials of matroid polytopes and polymatroids*, Discrete Comput. Geom. **42** (2009), no. 4, 670–702. [1](#)
- [10] Jesús A. De Loera, Raymond Hemmecke, and Matthias Köppe, *Algebraic and Geometric Ideas in the Theory of Discrete Optimization*, MOS-SIAM Series on Optimization, vol. 14, Society for Industrial and Applied Mathematics (SIAM), Philadelphia, PA; Mathematical Optimization Society, Philadelphia, PA, 2013. [3](#)
- [11] Eugène Ehrhart, *Sur les polyèdres rationnels homothétiques à n dimensions*, C. R. Acad. Sci. Paris **254** (1962), 616–618. [12](#)
- [12] Sophia Elia, Donghyun Kim, and Mariel Supina, *Techniques in equivariant Ehrhart theory*, Ann. Comb. **28** (2024), no. 3, 819–870. [1](#), [14](#), [15](#), [16](#)
- [13] Luis Ferroni and Akihiro Higashitani, *Examples and counterexamples in ehrhart theory*, EMS Surveys in Mathematical Sciences (2024). [9](#)
- [14] Vladimir Grujić, *Counting faces of graphical zonotopes*, Ars Math. Contemp. **13** (2017), no. 1, 227–234. MR 3669576 [2](#), [11](#)
- [15] John Shareshian and Michelle L. Wachs, *Eulerian quasisymmetric functions*, Adv. Math. **225** (2010), no. 6, 2921–2966. [15](#)
- [16] Richard P. Stanley, *Enumerative Combinatorics. Volume 1*, second ed., Cambridge Studies in Advanced Mathematics, vol. 49, Cambridge University Press, Cambridge, 2012. [12](#), [13](#)
- [17] Alan Stapledon, *Equivariant Ehrhart theory*, Advances in Mathematics **226** (2011), no. 4, 3622–3654. [1](#), [8](#), [13](#), [15](#)
- [18] John R. Stembridge, *Some permutation representations of Weyl groups associated with the cohomology of toric varieties*, Adv. Math. **106** (1994), no. 2, 244–301. [13](#), [15](#)